

Measuring Uncertainty in Transformer Circuits with Effective Information Consistency

Anatoly A. Krasnovsky^{1,2}

¹ Department of Computer Science and Engineering, Innopolis University, Russia

² MB3R Lab, Innopolis, 420500, Russia

Abstract. Mechanistic interpretability has identified functional subgraphs within large language models (LLMs), known as Transformer Circuits (TCs), that appear to implement specific algorithms. Yet we lack a formal, single-pass way to quantify when an *active* circuit is behaving coherently and thus likely trustworthy. Building on prior systems-theoretic proposals, we specialize a sheaf/cohomology and causal emergence perspective to TCs and introduce the *Effective-Information Consistency Score (EICS)*. EICS combines (i) a *normalized sheaf inconsistency* computed from local Jacobians and activations, with (ii) a *Gaussian EI proxy* for circuit-level causal emergence derived from the same forward state. The construction is white-box, single-pass, and makes units explicit so that the score is dimensionless. We further provide practical guidance on score interpretation, computational overhead (with fast and exact modes), and a toy sanity-check analysis. Empirical validation on LLM tasks is deferred.

Keywords: Mechanistic interpretability · Transformer circuits · Sheaf theory · Causal emergence · Uncertainty quantification · Large Language Models (LLMs)

1 Introduction

A central ambition in mechanistic interpretability is to reverse-engineer LLMs into meso-scale algorithmic components (“transformer circuits”) [10,1]. These subgraphs (attention heads, MLPs, and their pathways) have been linked to tasks such as copy/induction [10] and factual recall [15]. Once a circuit is identified, a natural question is: *is it functioning coherently on this input?* The same model may answer a factual prompt correctly or hallucinate; we hypothesize that the active circuit’s *causal integrity* differs between these regimes.

We build on sheaf-theoretic and causal-emergence ideas [7,4,11,12,13,9], instantiating them for transformer circuits. Our contribution is an *operational* metric, EICS, that can be computed from a single forward pass. Conceptually, uncertainty is treated as a failure of causal integrity: high emergence with low internal inconsistency suggests confidence; the opposite suggests risk. Unlike black-box UQ [2,3,8,14], EICS attributes uncertainty to specific *mechanisms*.

2 Related Work

Mechanistic interpretability. Induction heads and in-context learning behaviors were documented by Olsson et al. [10]. Recent “attribution graphs” tools (a.k.a. circuit tracing) provide subgraph discovery and validation pipelines [1]. Knowledge-related circuits are actively studied [15], and the relation between localization and editing has been scrutinized [5].

Uncertainty quantification (UQ). Black-box UQ includes distribution-free conformal prediction [2], calibration post-processing [3], deep ensembles [8], and Bayesian/approximate Bayesian methods for LLM finetuning such as Laplace-LoRA [14]. Our aim is complementary: a *white-box* signal grounded in the internal circuit.

Sheaves and causal emergence. Cellular sheaves provide a language for stitching local linear maps into globally consistent states; disagreement is measured via coboundaries and Hodge Laplacians [11,4]. Causal emergence quantifies when macroscale descriptions carry more effective information than parts [12,13,9]. We adapt these ingredients to transformer circuits with explicit, computable proxies.

3 Preliminaries

3.1 Transformer circuits

Let the transformer be a directed acyclic graph (DAG) $G = (V, E)$ with vertices as heads/MLPs and edges for information flow. A TC is a subgraph $G_M \subseteq G$ hypothesized to implement a task. For an input x , each $v \in V_M$ has activation $a_v \in \mathbb{R}^{d_v}$. We will write $e = (u \rightarrow v)$ for an oriented edge and use local linearizations at the observed activations.

3.2 Cellular sheaves on graphs and a computable inconsistency

We place a cellular sheaf \mathcal{F} on the *underlying undirected* version of G_M (so that 1-cochains live on edges regardless of the DAG’s direction), with stalks $\mathcal{F}(v) = \mathbb{R}^{d_v}$ and restriction maps on oriented edges given by the Jacobians evaluated at the current state:

$$\rho_e : \mathcal{F}(u) \rightarrow \mathcal{F}(v), \quad \rho_{u \rightarrow v} := J_{u \rightarrow v} \equiv \left(\frac{\partial f_v}{\partial a_u} \right)_a.$$

For a 0-cochain (node assignment) $s = \{s_v\}$, the sheaf coboundary $\delta^0 : C^0 \rightarrow C^1$ acts by

$$(\delta^0 s)_{(u \rightarrow v)} = \rho_{u \rightarrow v} s_u - s_v. \tag{1}$$

On a graph (no 2-cells), $\delta^1 = 0$, hence $H^1 \cong C^1 / \text{im } \delta^0$. Rather than taking a non-canonical “norm of a quotient,” we use a *normalized inconsistency energy*

from the observed activations $a = \{a_v\}$:

$$C_{\text{sh}}(G_M, a) = \frac{\left(\sum_{(u \rightarrow v) \in E_M} \|\rho_{u \rightarrow v} a_u - a_v\|_2^2\right)^{1/2}}{\varepsilon + \left(\sum_{(u \rightarrow v) \in E_M} \|a_u\|_2^2 + \|a_v\|_2^2\right)^{1/2}}, \quad (2)$$

with small $\varepsilon > 0$ for numerical stability. This is dimensionless and equals 0 iff a is a (noisily) consistent global section. One can optionally replace a by the least-squares projection $\hat{s} = \arg \min_s \sum_e \|\rho_e s_u - s_v\|^2$; both are single-pass (VJP/JVP-based) computations.

Node-seeded JVP computation (efficiency). To evaluate (2) efficiently, we use a *node-seeded* JVP scheme: for each source node $u \in V_M$ we perform a single JVP with seed a_u to evaluate all outgoing residual terms $\rho_{u \rightarrow v} a_u$ in one pass. This reduces the complexity from per-edge JVPs to $O(|V_M|)$ JVPs (typically 10–20 for medium circuits), while preserving the exact definition in (2).

3.3 A single-pass, Gaussian EI proxy

True effective information (EI) is intervention-defined. To obtain a single-pass proxy, we assume small, isotropic local interventions at the current state and approximate each map by its Jacobian. For a linear map $y = Jx + \xi$ with unit-variance isotropic x and small additive noise ξ , the mutual information (in nats) is proportional to $\frac{1}{2} \log \det(I + \alpha J^\top J)$ for scale $\alpha > 0$. We therefore define

$$\text{EI}_G(J) := \frac{1}{2} \log \det(I + \alpha J^\top J), \quad \Delta \text{EI}_G(G_M) := \text{EI}_G(J_M) - \sum_{v \in V_M} \text{EI}_G(J_v), \quad (3)$$

where J_M is the macro-Jacobian from the circuit’s inputs to its outputs (obtained by linearizing the composed subgraph). We use the positive part $\Delta \text{EI}_G^+ = \max(0, \Delta \text{EI}_G)$, and an optional normalization $\widehat{\Delta \text{EI}_G} := \Delta \text{EI}_G^+ / (\varepsilon + \text{EI}_G(J_M))$ to keep scores in $[0, 1)$.

3.4 Gaussian EI Proxy — Derivation and Implementation Notes

Setup. Consider a local, linearized description of a circuit around the observed forward state. Let $x \in \mathbb{R}^n$ denote a small stochastic intervention at the circuit inputs, and let $y \in \mathbb{R}^m$ be the circuit outputs. We approximate

$$y = Jx + \xi, \quad x \sim \mathcal{N}(0, \sigma_x^2 I_n), \quad \xi \sim \mathcal{N}(0, \sigma_\xi^2 I_m). \quad (4)$$

Mutual information. For a linear Gaussian channel with independent Gaussian input and noise,

$$I(x; y) = \frac{1}{2} \log \det\left(I_m + \frac{\sigma_x^2}{\sigma_\xi^2} J J^\top\right) = \frac{1}{2} \log \det\left(I_n + \frac{\sigma_x^2}{\sigma_\xi^2} J^\top J\right). \quad (5)$$

Proxy definition. We use the Gaussian EI proxy from Eq. (3); for a circuit G_M the emergence and its normalized positive part are, as in §3.3,

$$\widetilde{\Delta\text{EI}}_G = \frac{\max(0, \Delta\text{EI}_G)}{\varepsilon + \text{EI}_G(J_M)}. \quad (6)$$

Invariance, sensitivity, and small- α approximation. $\text{EI}_G(J)$ depends only on the singular values of J . Its sensitivity to α is

$$\frac{\partial}{\partial \alpha} \left(\frac{1}{2} \log \det(I + \alpha J^\top J) \right) = \frac{1}{2} \text{tr}[(I + \alpha J^\top J)^{-1} J^\top J],$$

and for $\alpha \sigma_{\max}^2 \ll 1$,

$$\frac{1}{2} \log \det(I + \alpha J^\top J) \approx \frac{\alpha}{2} \|J\|_F^2.$$

Computation. Use Cholesky/eigendecomposition for small n ; for larger n , use Hutch++/Lanczos log-det estimators with only JVP/VJP products. Residual connections can be handled by building the linearized block operator or evaluating log-det via Krylov methods.

4 Method: EICS

Given G_M , activations a , and edge Jacobians $\{\rho_{u \rightarrow v}\}$ from a single forward pass, we define

$$\text{EICS}(G_M; a) = \frac{\widetilde{\Delta\text{EI}}_G(G_M)}{1 + C_{\text{sh}}(G_M, a)}. \quad (7)$$

High EICS indicates (i) strong macro-level information integration relative to parts and (ii) low internal disagreement across edges.

Why this fixes earlier issues. (1) We never take a norm of a quotient space H^1 ; we measure *disagreement energy* (2) directly and dimensionlessly. (2) The EI term is a clearly stated Gaussian-logdet proxy; units are nats and become dimensionless via normalization. (3) DAGs have no directed cycles, but sheaf inconsistency remains meaningful on the undirected 1-skeleton.

Practical use and interpretation. By construction $C_{\text{sh}} \geq 0$ and $\widetilde{\Delta\text{EI}}_G \in [0, 1)$, hence $\text{EICS} \in [0, 1)$. Use a development split to select a threshold τ (AU-ROC/F1) and also report the components $1/(1 + C_{\text{sh}})$ and $\widetilde{\Delta\text{EI}}_G$ to diagnose drivers. For α , either set $\alpha = 1$ (SNR prior) or choose α to keep $\frac{1}{2} \log \det(I + \alpha J_M^\top J_M)$ in a target IQR to avoid saturation.

5 Theoretical properties

Assumption 1 (Local linearity and boundedness). *Along G_M , the maps are locally linear with Jacobians $\{\rho_e\}$ Lipschitz in a neighborhood of a , and operator norms are bounded. The sheaf Hodge Laplacian $L = \delta^{0\dagger}\delta^0$ (with the inner product induced by edge weights) has spectral gap $\lambda_2(L) > 0$ [4].*

Proposition 1 (Single-pass computability). *Under Assumption 1, both $C_{\text{sh}}(G_M, a)$ and $\widetilde{\Delta\text{EI}}_G(G_M)$ are deterministic functions of a single forward pass and its Jacobian-vector products. Consequently, EICS is $O(1)$ in the number of forward passes.*

Sketch. δ^0 is built from $\{\rho_e\}$ evaluated at a . Both the residual (2) and log-det terms (3) are functions of these objects. No Monte Carlo over inputs is required.

Proposition 2 (Stability to small off-circuit perturbations (bound)). *Let y denote circuit outputs. Consider an additive off-circuit perturbation η that couples into G_M with gain at most γ in operator norm. Under Assumption 1,*

$$\|\hat{s} - s^*\| \leq \frac{\gamma}{\lambda_2(L)} \|\eta\|, \quad \|\Delta y\| \leq \kappa \|\hat{s} - s^*\|$$

for a local Lipschitz constant κ . In particular, small C_{sh} (implying a large effective $\lambda_2(L)$) yields tighter bounds.

On the role of $\lambda_2(L)$. The bound scales with $1/\lambda_2(L)$ (Fiedler value). In practice $\lambda_2(L)$ depends on (i) connectivity and (ii) edge weights induced by local Jacobians. We recommend: (a) *report $\lambda_2(L)$ per circuit*; (b) *normalize edge weights* by operator norms of $\rho_{u \rightarrow v}$; and (c) optionally regularize $L \leftarrow L + \beta I$ when empirical $\lambda_2(L)$ is near-zero—tightening the practical bound without changing C_{sh} or EICS.

6 Algorithm

Computational overhead & scaling

Order-of-magnitude. With node-seeded JVPs, computing C_{sh} requires $O(|V_M|)$ JVPs (about 10–20 for medium circuits). In *fast* EI mode (small- α Frobenius approximation + Hutchinson-style probes), total autograd work is typically ~ 50 – 200 JVP/VJP products over the restricted subgraph, or about ~ 2 – 6 forward-equivalents. In *exact* EI mode (larger α or explicit factorizations), expect ~ 5 – 15 forward-equivalents. There is no input-level Monte Carlo; all quantities are deterministic functions of one forward state.

Scaling knobs. (a) Batch JVP seeds across nodes; (b) restrict EI to top- k singular directions via Lanczos; (c) cache intermediate linears along the TC; (d) prefer small- α for ranking tasks.

Algorithm 1 Single-pass EICS for a transformer circuit

- 1: **Input:** Model \mathcal{M} , input x , circuit $G_M = (V_M, E_M)$, scale $\alpha > 0$
 - 2: **Output:** $\text{EICS}(G_M; a)$
 - 3: **Forward & activations:** Run $\mathcal{M}(x)$ and record $\{a_v\}_{v \in V_M}$.
 - 4: **Edge Jacobians:** For each $(u \rightarrow v) \in E_M$, compute $\rho_{u \rightarrow v} = (\partial f_v / \partial a_u)_a$ via VJP/JVP.
 - 5: **Sheaf inconsistency:** Compute $C_{\text{sh}}(G_M, a)$ using (2). *Implementation:* Use *node-seeded JVPs* (one JVP per source node u) to evaluate all $\rho_{u \rightarrow v} a_u$ for outgoing edges.
 - 6: **Gaussian EI proxy:** Build macro-Jacobian J_M and node Jacobians $\{J_v\}$. Compute $\widetilde{\Delta\text{EI}}_G$ via (3).
 - Fast mode (ranking):** small- α approximation; Hutch++/Lanczos with 4-8 probes per J_v and 8-12 for J_M .
 - Exact mode (small blocks):** compute $\log \det(I + \alpha J^\top J)$ via Cholesky/SVD.
 - 7: **Score:** Return $\text{EICS} = \widetilde{\Delta\text{EI}}_G / (1 + C_{\text{sh}})$.
-

7 Proposed Validation

We outline an evaluation protocol for a factual QA task using an attribution-graph workflow [1] to identify a fact-retrieval circuit G_{fact} . Two sets are proposed: (A) questions with verifiable answers; (B) adversarial or hallucination-inducing prompts [6]. The expectation is higher EICS for set A (low C_{sh} , positive $\widetilde{\Delta\text{EI}}_G$) and depressed scores for set B. Comparators include log-prob/entropy, deep-ensemble variance [8], and conformal set sizes [2].

7.1 Baselines and ablations

(B1) Edge Activation Correlation (EAC). Average Pearson correlation between a_u and a_v across $(u \rightarrow v) \in E_M$ (dimension-wise).

(B2) Edge Alignment Residual (EAR). $\frac{1}{|E_M|} \sum_{(u \rightarrow v)} \|\hat{\rho}_{u \rightarrow v} a_u - a_v\|_2$ with per-edge least-squares $\hat{\rho}_{u \rightarrow v}$ (no sheaf coupling).

Ablations. (A1) $1/(1 + C_{\text{sh}})$ only; (A2) $\widetilde{\Delta\text{EI}}_G$ only.

7.2 Toy sanity-check (analytical & simulation protocol)

Setup. A 6-node feedforward TC with linear blocks and additive Gaussian edge noise; vary noise on a subset of edges. Compute C_{sh} , $\widetilde{\Delta\text{EI}}_G$ (fast/exact), EICS, and baselines across seeds.

Analytical sanity (small- α). With $\alpha = \sigma_x^2 / \sigma_\xi^2$, increasing additive noise reduces EI terms; edge noise increases residuals in (2). Hence EICS decreases with noise, matching intuition. See Fig. 1 for a synthetic sanity-check illustrating these trends.

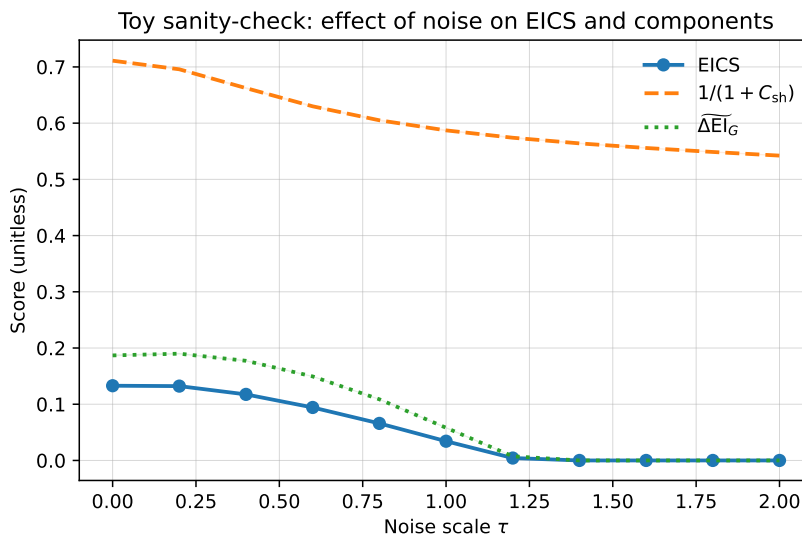


Fig. 1. Toy sanity-check on a 6-node circuit with two parallel branches. As node-noise τ increases, the sheaf inconsistency C_{sh} rises (so $1/(1 + C_{sh})$ falls). We also reduce cross-branch alignment with τ (edge decoherence), causing the emergence proxy $\widetilde{\Delta EI}_G$ and the overall EICS to decrease. Curves show means over seeds (no error bands for clarity). Definitions follow Eqs. (2), (3), and (7).

8 Discussion & limitations

Circuit dependency. EICS is only as meaningful as the specified G_M . **Linearization.** The Jacobian-based sheaf and EI proxy assume local linearity. **Cost.** Node-seeded JVPs, fast log-det, and top- k directions mitigate overhead. **Role with black-box UQ.** EICS provides *mechanistic* evidence complementing calibration/conformal tools.

9 Conclusion

We instantiate a sheaf-theoretic and causal-emergence perspective on transformer circuits as a practical, single-pass score (EICS). By replacing ill-posed cohomology norms with a normalized disagreement energy and adopting a Gaussian log-det EI proxy, EICS is both computable and dimensionless. We add practical guidance, computational cost analysis with fast/exact modes, and a toy sanity-check; full empirical validation follows the proposed protocol.

A Toy Sanity-Check Code for Fig. 1

The script below reproduces Fig. 1. It implements the two-branch toy circuit, computes C_{sh} (Eq. (2)), the normalized emergence proxy $\widetilde{\Delta EI}_G$ (Eqs. (3)), and EICS (Eq. (7)) as functions of the noise scale τ .

```

1 # Minimal toy-plot script for Fig. "Toy sanity-check"
2 # Requires: numpy, matplotlib. Saves: fig_toy_noise_curve.pdf
3 import numpy as np, matplotlib.pyplot as plt
4 EPS, D, N_SEEDS = 1e-8, 32, 100
5 TAUS = np.linspace(0.0, 2.0, 11)
6 alpha, align = 1.0, 0.9 # fixed SNR; high initial branch alignment
7
8 def rand_matrix(d, scale=0.8, rng=None):
9     rng = np.random.default_rng() if rng is None else rng
10    return scale * rng.normal(size=(d, d)) / np.sqrt(d)
11
12 def ei_proxy(J, alpha): # 0.5 * sum log(1 + alpha * sigma^2)
13    s = np.linalg.svd(J, compute_uv=False)
14    return 0.5 * np.sum(np.log1p(alpha * (s**2)))
15
16 def build_branch_mats(D=32, align=0.9, rng=None):
17    rng = np.random.default_rng(123) if rng is None else rng
18    U = rand_matrix(D, 0.8, rng); A = rand_matrix(D, 0.9, rng); W =
19        rand_matrix(D, 0.9, rng)
20    W13 = U; W23 = (1-align)*rand_matrix(D,0.8,rng) + align*U
21    W34 = A; W35 = (1-align)*rand_matrix(D,0.9,rng) + align*A
22    W46 = W; W56 = (1-align)*rand_matrix(D,0.9,rng) + align*W
23    return W13, W23, W34, W35, W46, W56
24
25 def metrics_at_tau(tau, rng):
26    W13,W23,W34,W35,W46,W56 = build_branch_mats(D, align, rng)
27    # Edge decoherence: reduce cross-branch alignment as tau grows
28    h = min(1.0, tau/2.0)
29    nrg = np.random.default_rng(rng.integers(10**9))
30    W56 = (1-h)*W56 + h*rand_matrix(D, 0.9, nrg)
31    W35 = (1-h)*W35 + h*rand_matrix(D, 0.9, nrg)
32
33    # Two parallel subpaths (parts), macro map is their sum
34    Jb1 = W46 @ W34 @ W13
35    Jb2 = W56 @ W35 @ W23
36    JM = Jb1 + Jb2
37
38    EI_macro = ei_proxy(JM, alpha)
39    EI_parts = ei_proxy(Jb1, alpha) + ei_proxy(Jb2, alpha)
40    dEI_g = max(0.0, EI_macro - EI_parts) / (EPS + EI_macro)
41
42 # Activations for C_sh with node noise
43 a1 = rng.normal(size=D); a2 = rng.normal(size=D)
44 a3 = W13@a1 + W23@a2; a4 = W34@a3; a5 = W35@a3; a6 = W46@a4 + W56@a5

```

```

44 a1o = a1 + tau*rng.normal(size=D); a2o = a2 + tau*rng.normal(size=D)
45 a3o = a3 + tau*rng.normal(size=D); a4o = a4 + tau*rng.normal(size=D)
46 a5o = a5 + tau*rng.normal(size=D); a6o = a6 + tau*rng.normal(size=D)
47
48 edges = [(a1o,a3o,W13),(a2o,a3o,W23),(a3o,a4o,W34),
49           (a3o,a5o,W35),(a4o,a6o,W46),(a5o,a6o,W56)]
50 num = den = 0.0
51 for au,av,W in edges:
52     r = W@au - av; num += r@r; den += au@au + av@av
53 Csh = np.sqrt(num) / (EPS + np.sqrt(den))
54 EICS = dEI_g / (1.0 + Csh)
55 return Csh, dEI_g, EICS
56
57 # Sweep tau and average over seeds
58 C_m, d_m, S_m = [], [], []
59 C_e, d_e, S_e = [], [], []
60 for tau in TAUS:
61     Cs, ds, Ss = [], [], []
62     for k in range(N_SEEDS):
63         rng = np.random.default_rng(1000 + k)
64         Csh, dEIg, EICS = metrics_at_tau(tau, rng)
65         Cs.append(Csh); ds.append(dEIg); Ss.append(EICS)
66     Cs, ds, Ss = map(np.array, (Cs,ds,Ss))
67     C_m.append(Cs.mean()); d_m.append(ds.mean()); S_m.append(Ss.mean())
68     C_e.append(Cs.std(ddof=1)/np.sqrt(N_SEEDS))
69     d_e.append(ds.std(ddof=1)/np.sqrt(N_SEEDS))
70     S_e.append(Ss.std(ddof=1)/np.sqrt(N_SEEDS))
71
72 # Plot (one panel; PDF for LNCS)
73 TAUS = np.array(TAUS); C_m=np.array(C_m); d_m=np.array(d_m); S_m=np.array(
74     S_m)
75 C_e=np.array(C_e); d_e=np.array(d_e); S_e=np.array(S_e)
76 plt.figure(figsize=(6.2,4.2))
77 plt.plot(TAUS, S_m, '-o', label='EICS')
78 invC = 1.0/(1.0 + C_m)
79 plt.plot(TAUS, invC, '--', label=r'$1/(1+C_{\mathrm{sh}})$')
80 plt.plot(TAUS, d_m, ':', label=r'$\widetilde{\Delta}_{\mathrm{EI}}_G$')
81 plt.xlabel(r'Noise scale $\tau$'); plt.ylabel('Score (unitless)')
82 plt.title('Toy sanity-check: effect of noise on EICS and components')
83 plt.grid(True, linewidth=0.5, alpha=0.5); plt.legend(frameon=False)
84 plt.tight_layout(); plt.savefig('fig_toy_noise_curve.pdf', bbox_inches=
85     'tight')

```

References

1. Circuit tracing / attribution graphs: Methods & applications (2025), <https://transformer-circuits.pub/2025/attribution-graphs/>

2. Angelopoulos, A.N., Bates, S.: A gentle introduction to conformal prediction and distribution-free uncertainty quantification (2021), <https://arxiv.org/abs/2107.07511>
3. Guo, C., Pleiss, G., Sun, Y., Weinberger, K.Q.: On calibration of modern neural networks. In: Proceedings of the 34th International Conference on Machine Learning (ICML). pp. 1321–1330. PMLR (2017)
4. Hansen, J., Ghrist, R.: Toward a spectral theory of cellular sheaves **3**(4), 315–358 (2019)
5. Hase, P., Bansal, M., Kim, B., Ghandeharioun, A.: Does localization inform editing? surprising differences in causality-based localization vs. knowledge editing in language models. In: Advances in Neural Information Processing Systems (NeurIPS). vol. 36, pp. 17643–17668 (2023)
6. Huang, L., Yu, W., Ma, W., Zhong, W., Feng, Z., Wang, H., Chen, Q., Peng, W., Feng, X., Qin, B., et al.: A survey on hallucination in large language models: Principles, taxonomy, challenges, and open questions **43**(2), 1–55 (2025)
7. Krasnovsky, A.A.: Sheaf-theoretic causal emergence for resilience analysis in distributed systems (2025), <https://arxiv.org/abs/2503.14104>
8. Lakshminarayanan, B., Pritzel, A., Blundell, C.: Simple and scalable predictive uncertainty estimation using deep ensembles. In: Advances in Neural Information Processing Systems (NeurIPS). vol. 30 (2017)
9. Oizumi, M., Albantakis, L., Tononi, G.: From the phenomenology to the mechanisms of consciousness: Integrated information theory 3.0 **10**(5), e1003588 (2014)
10. Olsson, C., Elhage, N., Nanda, T., Joseph, N., DasSarma, N., Henighan, T., Mann, B., Askell, A., Bai, Y., Chen, A., et al.: In-context learning and induction heads (2022), <https://arxiv.org/abs/2209.11895>
11. Robinson, M.: Topological Signal Processing. Springer (2014)
12. Rosas, F.E., Mediano, P.A.M., Jensen, H.J., Seth, A.K., Barrett, A.B., Carhart-Harris, R.L., Bor, D.: Reconciling emergences: An information-theoretic approach to identify causal emergence in multivariate data **16**(12), e1008289 (2020)
13. Tononi, G., Sporns, O.: Measuring information integration **4**, 31 (2003)
14. Yang, A.X., Robeyns, M., Wang, X., Aitchison, L.: Bayesian low-rank adaptation for large language models (laplace-lora) (2023), <https://arxiv.org/abs/2308.13111>, iCLR 2024 version
15. Yao, Y., Zhang, N., Xi, Z., Wang, M., Xu, Z., Deng, S., Chen, H.: Knowledge circuits in pretrained transformers. In: Advances in Neural Information Processing Systems (NeurIPS). vol. 37, pp. 118571–118602 (2024)